

Article

RSS/TDoA-Based Source Localization in Microwave UWB Sensors Networks Using Two Anchor Nodes [†]

Sergei Ivanov ^{*}, Vladimir Kuptsov , Vladimir Badenko  and Alexander Fedotov 

Institute of Electronics and Telecommunications, Peter the Great St. Petersburg Polytechnic University, 29 Polytechnicheskaya Str., 195251 Saint Petersburg, Russia; kuptsov@spbstu.ru (V.K.); badenko_vl@spbstu.ru (V.B.); afedotov@spbstu.ru (A.F.)

* Correspondence: ivanov_si@spbstu.ru; Tel.: +7-905-283-48-88

[†] The paper is an extension of conference. Presented at the Intelligent Information Technology and Mathematical Modeling 2021 (IITMM 2021) Divnomorskoe, Krasnodar Territory, Russia, 30 May–6 June 2021.

Abstract: The manuscript presents an algorithm for the optimal estimation of the amplitude and propagation delay time of an ultra-wideband radio signal, in systems for the passive location of fixed targets based on the hybrid RSS/TDoA method in two-dimensional space with two base stations. The optimal estimate is based on the Bayesian strategy of maximum a posteriori probability density, taking into account a priori data on the statistical properties of the Line of Sight radio channel during Gaussian monocycle propagation. The Bayesian Cramer–Rao lower bound (BCRLB) of the delay time and the amplitude estimates for a time-discrete signal are calculated, and the resulting parameter estimate is compared with BCRLB. An algorithm has been developed for optimal estimation of distances from the radiation source to base stations, based on the results of the measurements of the amplitude and the propagation delay time of the UWB radio signal. The calculation of the statistical characteristics of the obtained estimate is carried out, and the functional dependence of the characteristics on various parameters is analyzed.

Keywords: localization; UWB Networks; maximum likelihood (ML) estimator; received signal strength (RSS); time difference of arrival (TDOA)



Citation: Ivanov, S.; Kuptsov, V.; Badenko, V.; Fedotov, A. RSS/TDoA-Based Source Localization in Microwave UWB Sensors Networks Using Two Anchor Nodes. *Sensors* **2022**, *22*, 3018. <https://doi.org/10.3390/s22083018>

Academic Editor: David Plets

Received: 1 March 2022

Accepted: 12 April 2022

Published: 14 April 2022

Publisher's Note: MDPI stays neutral with regard to jurisdictional claims in published maps and institutional affiliations.



Copyright: © 2022 by the authors. Licensee MDPI, Basel, Switzerland. This article is an open access article distributed under the terms and conditions of the Creative Commons Attribution (CC BY) license (<https://creativecommons.org/licenses/by/4.0/>).

1. Introduction

The coordinates determination of a radio emission source using Microwave Sensors Networks (MSNs) is widely used in devices for various applications, including environmental monitoring, intelligent transportation, precision agriculture, smart home, medicine, and others [1–5]. For some sensor nodes, called anchor nodes (AN) (base stations), spatial coordinates are known in some positioning system. The location coordinates of the remaining nodes, called source nodes (SN), are estimated using various positioning algorithms, usually based on measuring radio signal parameters [1,6].

At present, several efficient methods for the spatial positioning of radio sources using MSNs have been developed. These include the following positioning techniques:

- time of arrival (TOA) [7–9],
- time-difference-of-arrival (TDOA) [2,10,11],
- direction of arrival (DOA) or angle of arrival (AOA) [1],
- received signal strength (RSS) indicator [12–14].

Each of the listed positioning techniques has its advantages and disadvantages and is used to solve specific problems in given conditions. It is effective to combine several positioning techniques, for example, TDOA and FDOA [15] or TDOA and AOA [16]. In this work, we analyze a hybrid method for positioning a quasi-stationary radio source using TDOA/RSS algorithms for processing measurements.

When the location system is operating in RSS mode, the power P or amplitude A of the signal emitted by the source is measured at the input of the base station receiver. In a

real radio channel, the signal level is attenuated due to three factors: large-scale path loss, multipath fading, and shadowing [17]. In free space, large-scale path loss is a deterministic function of the distance between transmitter (Tr) and receiver (Rv), proportional to r^{-2} , where r is the distance between Tr and Rv. Multipath fading is caused by interference at the receiving point of several copies of the transmitted signal Tr that are delayed for different times. One effective way to deal with multipath fading is to use ultra wideband (UWB) pulsed radio systems, due to their high time resolution capability [18]. However, UWB technology is not yet fully developed, and efficient design of such communication systems requires new experimental and theoretical studies. In particular, it is necessary to develop a statistical channel model that adequately describes the propagation of a UWB signal under various conditions, but, at the same time, it should be simple enough to make theoretical analysis and computer simulation possible. The use of such an analytical model (in a closed form), for constructing a localization algorithm and calculating the statistical characteristics of estimating the position of a radio source using MSNs, is not currently described in the literature.

As confirmed by numerous studies, the most-tested statistical model that reflects the small-scale properties of the UWB channel, including in indoor spaces with small volume, is the modified Saleh–Valenzuela parametric model [18], which, as it turned out, corresponded best of all to the experimental data [19–22].

Statistical small-scale properties of a discrete internal radio channel are reflected by the impulse response $h(t)$, which for the modified Saleh–Valenzuela model has the form [23,24].

$$h(t) = X \sum_{l=1}^L \sum_{k=1}^K \beta_{k,l} \delta(t - T_l - \tau_{k,l}), \quad (1)$$

where T_l is the signal propagation time delay of the l -th cluster, $\beta_{k,l}$ and $\tau_{k,l}$ are the amplitude and arrival delay of the k -th ray in the l -th cluster, L is the number of clusters, and K is the maximum number of rays in the cluster. Time delays T_l and $\tau_{k,l}$ are described by a Poisson process, while the random variable X is called the shading factor and is described by a lognormal distribution with a standard deviation σ_X , called the shading depth.

Numerous studies have shown that for the amplitude $\beta_{k,l}$, the lognormal or Nakagami distributions provide the best of all correspondence to the experimental data [23–25]. As follows from (1), the statistical characteristics of the UWB channel of MSNs differ significantly from the characteristics of a narrowband channel. There are also some peculiarities of the propagation of UWB signals at indoor spaces with small volume. We will use the statistical properties of $h(t)$ to develop an algorithm for efficient estimation of the spatial position of SN and to calculate the Cramer–Rao lower bound for this estimation.

In [7,26,27], the results of the positioning coordinates estimation obtained by the TDoA and RSS methods are compared. It is shown that the efficiency of TDoA-based systems increases when using UWB signals and signals with a large base (the product of duration and signal bandwidth). However, TDoA positioning errors increase dramatically when MSNs are operated indoors, where source signal undetectable direct path (UDP) conditions occur due to the presence of a large number of NLOS channels or a large attenuation of the signal when it propagates along the LOS channel. The efficiency of RSS-based systems is less sensitive to operating conditions in large-scale path loss, multipath fading, and shadowing modes, but signal strength estimation methods have large errors.

In works [28–31], in contrast to existing studies, in which it was assumed that the TDOA measurement noise variance was independent of the respective distances from the source to the sensor, a more realistic model was considered, in which the signal-to-noise ratio (SNR) is a function of the distance from the source to the sensor. The proposed hybrid TDoA/RSS methods improve the accuracy of source localization estimation compared to TDOA or RSS methods used separately. The gain of the hybrid TDoA/RSS method is especially noticeable in the proximity to the base stations but makes a small contribution at a low noise level. It is shown that the estimation accuracy of the proposed localization

algorithm is comparable to the Cramer–Rao lower bound (CRLB), taking into account moderate TDOA measurement noise. However, the results obtained in these works do not consider the specifics of UWB signals. The statistical properties of the signal propagation channel in MSNs are taken into account by the log-normal distribution of the integral (total) power of the received signal at the SN input. This does not take into account the multipath components of NLOS and LOS, and the First Detected Peak of the Direct Path channel is not determined.

A method for determining the coordinates of a radiation source in an indoor space, taking into account the decomposition of the signal in the statistical channel of MSNs into multipath components, was proposed in [32–34]. As part of the received signal at the SN input, the NLOS and LOS components are distinguished. Using the statistical properties of the signal propagation channel, the FDP is identified with the DP channel or the Undetected Direct Path (UDP) mode is registered. In the first case, the SN coordinates are determined by the FDP time position using the ToA or TDoA method; in the second case, we can talk about a possible large localization error. The proposed semi-empirical target localization technique makes it difficult to carry out a theoretical analysis of the statistical properties of the SN coordinate estimate, and, therefore, such an analysis is not carried out in the above works.

A large number of works are devoted to the development of methods for determining the type of the probability distribution function and estimating its parameters that describe the statistical properties of the propagation of signals (including ultra-wideband signals) in MSNs channels in indoor spaces (see, for example, [34–36]). The resulting estimates and properties of parameters and distributions are used to develop methods for efficient estimation of SN location coordinates.

The development of hybrid TDoA/RSS positioning methods using UWB signals for MSNs in indoor spaces has been the subject of many studies, and the results of some are presented in [37–45]. An analysis of these results shows that in the absence of a priori experimental data on the statistical characteristics of signal propagation channels in this particular heterogeneous environment, localization based on joint RSS/TDoA methods (strategies) is a complex problem that is difficult to solve without simplifying the mathematical model. For example, to obtain a strategy estimate for the maximum likelihood function or weighted least squares RWLS related to a non-convex optimization problem, a transformation to a convex optimization problem is used, which is then solved by methods of semi-definite programming SDP.

The objective of the study is based on the following statements. As the analysis of the results of the work shows, the problem of estimating the coordinates of the radiation source is solved by complex numerical calculations. The solution is multiparametric, but not all dependencies can be obtained and have a physical interpretation. At the same time, there is a practical need to use a small (minimal) number of ANs in MSNs. It is also possible to operate MSNs in conditions where the influence of NLOS channels on LOS channels is small, for example, when using UWB signals and the appropriate operating range of base station receivers. However, at the same time, the power and amplitude of the LOS channel signal components are random variables due to the statistical properties of the signal propagation medium.

Of current and practical interest is the consideration of the problem of developing a strategy for efficient coordinate estimation of the hybrid RSS/TDoA method for UWB Sensors Networks Using Two Anchor Nodes under conditions when the First Detected Peak of the AN receiver coincides with the DP channel component and the influence of the NLOS channel on the LOS channel can be neglected. It is assumed that the statistical properties of the LOS channel signal are described by a log-normal distribution.

Some results of this study were reported by the authors at a conference [46].

The structure of the paper is as follows. Section 2 of the article considers a description of the mathematical model of signals in TDOA/RSS location systems, which are analyzed in this paper. A mathematical model of a UWB radio pulse—a Gaussian monocycle

is presented, as well as the properties of the probability density of the logarithmically normal distribution of the signal amplitude during its propagation in a medium. Section 3 describes the Hybrid TDoA/RSS Estimator of propagation delay time and signal amplitude. Section 4 provides a derivation of the Cramer–Rao lower bound for the delay time and signal amplitude estimates. A description of the source distance estimator and its statistical characteristics are also given. Section 5 presents the results of a computational experiment for estimating the parameters. Finally, the concluding remarks and future works are presented in Section 6.

2. Problem Statement and System

Let us define the class of TDOA/RSS location systems, the analysis of which is carried out in this paper. Consider two base stations of the location system, one of which is the reference station. ANs (sensors) operate in the corporate synchronous mode of common time t , and their position is given by known coordinates $(x_i, y_i) i = 1, 2, \dots, P$, where P is the AN number in the location system (see Figure 1). ANs receive a radio signal $s(t')$ from a fixed-point source (S) with unknown coordinates (x, y) located at a distance r_i from the corresponding i -th base station (see Figure 1). We assume that the source emits a signal of a known function of time $s_0(t')$, the reference points of the time axes t and t' are shifted by an unknown value δt , and the operation of the source transmitter is asynchronous in time with the operation of the BS receivers. The mathematical model of received by AN signals $x_i(t)$ in discrete time is described by the following relationships:

$$s_0 = [s_0(t'_1), s_0(t'_2), \dots, s_0(t'_N)]^T, \tag{2}$$

$$s_i = [s_i(t'_1 - \tau_i), s_i(t'_2 - \tau_i), \dots, s_i(t'_N - \tau_i)]^T, \tag{3}$$

$$n_i = [n_i(t'_1), n_i(t'_2), \dots, n_i(t'_N)]^T, \tag{4}$$

$$x_i = [x_i(t'_1), x_i(t'_2), \dots, x_i(t'_N)]^T, \tag{5}$$

$$x_i = A_i s_i + n_i, \tag{6}$$

where s_0 is the source signal S; s_i is delayed by τ_i and attenuated signal of source S; x_i is input signal of the i -th sensor receiver; n_i is white Gaussian noise reduced to the input of the i -th sensor, uncorrelated with the source signal; and the symbol T means the vector transposition operation.

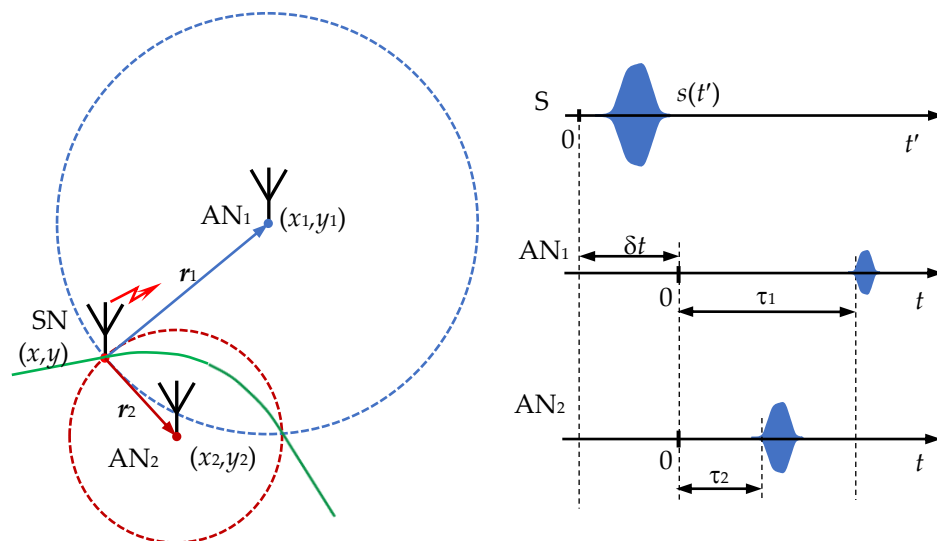


Figure 1. Block diagram of the TDoA/SSR-based positioning system.

The sampling interval $\Delta t = t_{k+1} - t_k$ is determined by the operating frequency range Δf of the emitted signal $s(t)$, with $\Delta t = 1/\Delta f$. Thus, at the observation time interval T_0 of the signal $x_i(t)$, the number of uncorrelated samples of the sample group and, accordingly, the dimension of the vectors is $1 \times N$, where $N = T_0/\Delta t = T_0\Delta f$. The probability density distribution of noise counts $n_i(t_k) = n_k$ is considered to be given $p_n(n_k) = \mathcal{N}(0, \sigma_n^2)$, i.e., noise samples n_k are statistically independent centered Gaussian random variables. Such a distribution class adequately describes the model of the impact of quasi-stationary noise inherent in the receiver itself, as well as other additive processes such as thermal noise at the receiver input. As a rule, the use of non-Gaussian noise models, for example, impulsive random processes, does not allow one to obtain a closed analytical form of optimal signal processing algorithms. This disadvantage makes it problematic to conduct transparent analysis when using very powerful statistical tools, such as maximum likelihood estimation and Bayesian estimation [47,48]. However, in some media, for example, for the ocean noise model, the use of non-Gaussian distributions is necessary [47].

The amplitude A_i of the wanted signal at the input of the i -th sensor is determined by the power of the source transmitter S and the law of attenuation of the electromagnetic wave in the location space. As noted above, we will take into account the statistical properties of the signal propagation medium in the approximation, when the influence of NLOS channels on LOS channels is small and the equation for the squared random value of the signal amplitude (power) is as follows:

$$10 \lg \frac{A_i^2}{A_0^2} = -10\gamma \cdot \lg r_i/r_0 + n_P, \quad (7)$$

where n_P —is a centered Gaussian random variable with $p_P(n_P) = \mathcal{N}(0, \sigma_P^2)$ probability density distribution. The reference power value A_0^2 in relation (7) is measured, for example, at a distance $r_0 = 1$ m from the source. In works [17,23,24], the values of coefficients σ_P^2 and γ of distribution (7) are given for different conditions of source signal propagation. The standard deviation (RMS) σ_P can reach 12 dB and the γ parameter ranges from 2 (free space) to 6 (for multipath propagation in a multicomponent environment, for example, indoors).

Relation (7) determines the log-normal distribution of the probability density of the amplitude A_i [49] with an average value $M\{A_i\}$

$$M\{A_i\} = A_0 \left(\frac{r_0}{r_i} \right)^{\frac{\gamma}{2}} \exp \left[\frac{1}{2} \frac{(\sigma_P)^2 (\ln 10)^2}{20} \right] = A_0 \left(\frac{r_0}{r_i} \right)^{\frac{\gamma}{2}} \exp \left(\frac{1}{2} \sigma_{Pe}^2 \right), \quad (8)$$

and variance $D\{A_i\}$ equal to [49]

$$D\{A_i\} = \sigma_{A_i}^2 = A_0^2 \left(\frac{r_0}{r_i} \right)^{\gamma} \exp(\sigma_{Pe}^2) \left[\exp(\sigma_{Pe}^2) - 1 \right], \quad (9)$$

For the case when the variance σ_{Pe}^2 of the normalized signal power is much less than one, the asymmetry and kurtosis coefficients of the probability density distribution of the parameter A_i are equal to a small value, and, therefore, the distribution law of the probability density of the amplitude $p(A_i)$ can be considered approximately normal [49].

$$p(A_i) = \frac{1}{\sqrt{2\pi\sigma_{A_i}^2}} \exp \left[-\frac{1}{2} \frac{(A_i - M\{A_i\})^2}{\sigma_{A_i}^2} \right], \quad (10)$$

Figure 2a shows the change in the random value of the amplitude A_i for various values of the parameter $\sigma_P = 6$ dB and 1.5 dB of the lognormal distribution. In the proposed model for describing the channel for the propagation of microwave signals in a medium, it is assumed that during the time interval when the amplitude A_i and the delay time τ are estimated, the values of these parameters remain unchanged. In the next measurement

session, with the same coordinates of the source SN, the amplitude A_i has a random value from the general population with a lognormal distribution. In Figure 2b, the probability distribution density (PDF) of the amplitude (b) for various values of the parameter σ_P of the lognormal distribution is shown. For σ_P variances less than 1.5 dB, the lognormal and normal (ND) distributions almost coincide. For large values of dispersion, the probabilistic interval of changes in the amplitude A_i with a lognormal distribution significantly exceeds the corresponding interval with a normal distribution of a random variable. This feature is explained by the flat “tails” of the lognormal distribution (see Figure 2b). Another feature of the lognormal distribution in accordance with relations (8) and (9) is the dependence of $M\{A_i\}$ and $D\{A_i\}$, simultaneously, on two distribution parameters σ_{Pe}^2 and μ_i .

$$\mu_i = \gamma \cdot \lg\left(\frac{r_0}{r_i}\right), \quad (11)$$

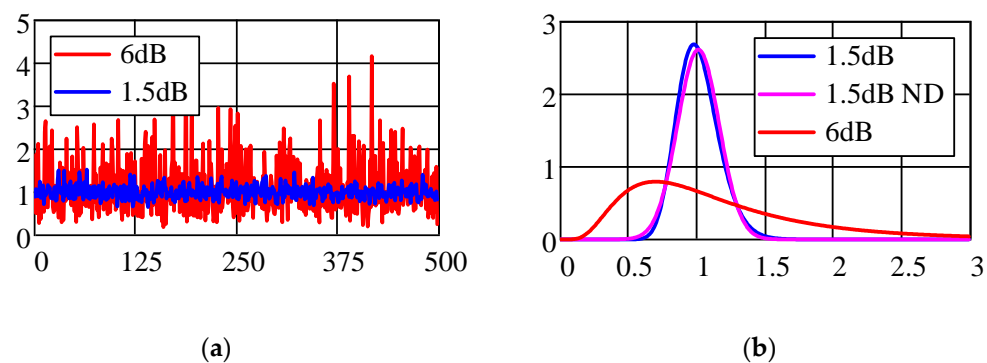


Figure 2. Change in the amplitude of the UWB signal (a) and the probability distribution density of the amplitude (b) for different values of the parameter σ_P of the lognormal distribution.

The impulse response of the channel is affected by the polarization of the radio wave and the radiation pattern of the receiving and emitted antennas. In this paper, these effects are not studied. It should also be noted that although the Saleh–Valenzuela model was developed for None Line of Sight (NLOS) channels, it has also been applied to Line of Sight (LOS) channels, where it is more limited [23].

As noted above, for the tasks of radar and navigation with short ranges and high spatial resolution, a promising direction is the use of UWB technologies. The main definitions and technical features of UWB technologies are given in [50,51]. To analyze the RSS/TDoA-Based Source Localization hybrid method being developed, we chose an ultra-short radio pulse as a Waveform UWB signal, for which the change in the envelope over time is described by the first derivative of the Gaussian function. The waveform of the envelope of the UWB signal and the module of the amplitude spectrum are shown in Figure 3. The envelope of the emitted signal $s_0(t)$ as a known function of time is described by the expression

$$s_0(t) = A_0 \frac{t}{\tau_0} \exp\left[-\left(\frac{t}{\tau_0}\right)^2\right] \text{rect}\left[\frac{t}{T} - \frac{1}{2}\right] = A_0 s(t), \quad (12)$$

In Formula (12), A_0 is the signal amplitude at the reference distance r_0 , which determines the pulse power of the emitted signal $P_0 \sim A_0^2/4$; τ is the parameter of the UWB pulse and T is effective pulse width. Not less than 99% is concentrated on the time interval T at $T = 4\tau_0$. The rectangular function $\text{rect}(x)$ (unit pulse) is expressed in a standard way in terms of the Heaviside function [52]. Figure 2a also shows the ‘mother’ Gaussian function (2), the derivative of which generates the shape of the envelope of the emitted signal.

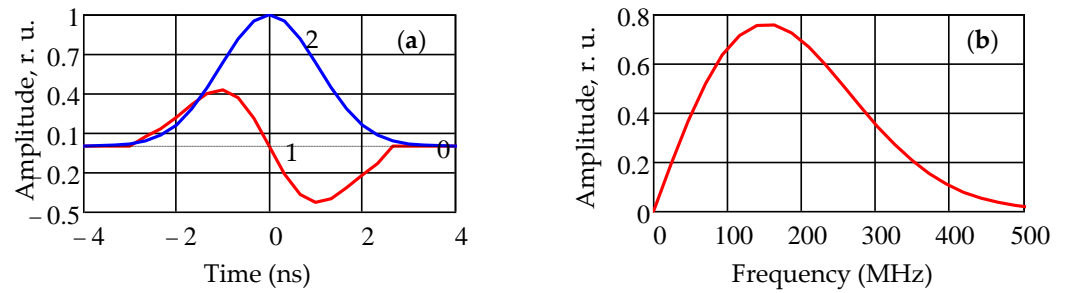


Figure 3. Waveform of the UWB signal (a) and the modulus of its amplitude spectrum (b).

Modern receiver modules use the technology of heterodyning and the IQ quadrature conversion of the input signal. In further analysis, it is assumed that the radio signal with the center frequency f_0 is converted into a signal during heterodyning, of which the mathematical model is described by relation (12). We also assume that the medium within the direct path of signal propagation is weakly dispersive in the frequency band of the operating range, and the distortions of the shape of the envelope (12) are small. It is assumed that the influence of the NLOS channels on the LOS channels is small due to the choice of a small parameter τ and, accordingly, the small duration of the interval T compared to the additional time delay in the NLOS channels. The introduced restrictions make it possible to develop an optimal algorithm for processing the received signal in the joint TDoA/RSS assessment mode.

3. The Proposed Hybrid TDoA/RSS Estimator

For further analysis, it is advisable in the mathematical model of the signal (1)–(5) to move from the space of discrete time to the space of discrete frequency ω_k . The signal spectrum sampling interval $\delta f = f_{k+1} - f_k$ is equal to $\delta f = \Delta f/N$, then $\omega_k = 2\pi f_k = 2\pi k \delta f$. After performing the DFT on the received signal $x(t)$, we obtain a complex-valued vector of the signal spectrum.

$$\tilde{X}_i = [\tilde{X}_i(f_1), \tilde{X}_i(f_2), \dots, \tilde{X}_i(f_N)]^T, \quad (13)$$

Similar expressions for the discrete spectrum can be written by performing the DFT on the signal $s(t)$ and the noise $n(t)$. Then, the mathematical model of the received signal can be represented as follows:

$$\tilde{X}_i = A_i \tilde{S}_i e^{-j\omega_k \tau_i} + \tilde{N}_i, \quad (14)$$

In Equation (13), the vector X has a multivariate complex normal distribution with mean $m(\theta)$ and covariance matrix K [53–55]

$$\mathcal{CN}(\tilde{m}_i(\theta), K), \quad (15)$$

and mathematical expectation.

$$\tilde{m}_i(\theta) = A_i \tilde{S}_i e^{-j\omega_k \tau_i}, \quad (16)$$

The covariance matrix K , in our case of statistically independent elements of the vector X_i , is expressed through the identity matrix.

$$K = \frac{N_0}{2} T_0 \cdot \mathbf{1}, \quad (17)$$

where $N_0/2$ is two-sided noise power spectral density $n(t)$, and $\theta = [A_i, \tau_i]^T$ is the vector of parameters to be estimated.

In most radio engineering problems, when estimating signal parameters, the maximum a posteriori density (MAPD) method (or the maximum a posteriori (MAP) esti-

mate) is mainly used [53,54]. The estimates obtained by the MAPD have a number of advantages—the comparative simplicity of calculations and the technical implementation of the corresponding optimal algorithms using modern digital processors. An important advantage of the MAP estimate is that the estimate is asymptotically efficient for a large sample size X_i [53,54].

For a complex vector sample X_i of statistically independent samples, the joint conditional probability distribution density $p_X(X_i | \theta)$ has the form [53,55].

$$p(X_i | \theta) = \frac{1}{\det[\pi\mathbf{K}]} \exp \left\{ - [\tilde{X}_i - \tilde{m}(\theta)]^H [\frac{1}{2}\mathbf{K}^{-1}] [\tilde{X}_i - \tilde{m}(\theta)] \right\}, \quad (18)$$

where \mathbf{K}^{-1} —is the inverse matrix of the covariance matrix \mathbf{K} . This is according to relation (15), in our case.

$$\mathbf{K}^{-1} = \frac{1}{T_0 N_0} \cdot \bar{\mathbf{1}}, \quad (19)$$

Bayesian MAP estimation seeks the maximum of the Bayesian log-likelihood function (log-likelihood function) [53,54].

$$l_B(\theta, \tilde{X}_i) = \ln p(\tilde{X}_i | \theta) + \ln p_\theta(\theta) + \zeta, \quad (20)$$

In our case, the form $p_\theta(\theta) = p_A(A_i)$ is determined by the relation for the lognormal distribution $\text{LogN}(\mu_i, \sigma_p^2)$ [49].

$$p_A(A_i) = \text{LogN}(i, \sigma_p^2) = \frac{M_1}{A_i \sigma_p \sqrt{2\pi}} \exp \left[-\frac{1}{2} \frac{(\log A_i - \mu_i)^2}{\sigma_p^2} \right] \text{ for } A_i > 0, \quad (21)$$

Parameter $M_1 = \lg(e)$; ζ —is a function independent of the vector parameter θ . In expression (21), for the Bayesian log-likelihood function $l_B(\theta, X)$, the first term takes into account the information obtained from the observation results and the second—a priori information.

The likelihood equation that determines the estimate of the vector parameter θ can be written in a compact form [53,54].

$$\nabla_\theta [l_B(\theta, \tilde{X}_i)]_{\theta=\hat{\theta}(\tilde{X})}, \quad (22)$$

where ∇_θ is the vector symbol of a multidimensional 2×1 gradient.

$$\nabla_\theta \triangleq \left[\frac{\partial}{\partial A_i}, \frac{\partial}{\partial i} \right]^T, \quad (23)$$

A more general algorithm for estimating the vector parameter θ has the form [53,54].

$$\theta(\tilde{X}) = \underset{\theta}{\text{argmax}} [l_B(\theta, \tilde{X}_i)], \quad (24)$$

Using the results obtained in [53,54], we obtain the following expressions for estimating the vector parameter θ .

$$\Re \left\{ \frac{\partial \tilde{m}^H(\theta)}{\partial A_i} \mathbf{K}^{-1} [\tilde{X}_i - \tilde{m}[\theta]] \right\}_{\theta=\hat{\theta}} + \frac{\partial p_A(A_i)}{\partial A_i}_{\theta=\hat{\theta}} = 0, \quad (25)$$

$$\Re \left\{ \frac{\partial \tilde{m}^H(\theta)}{\partial \tau_i} \mathbf{K}^{-1} [\tilde{X}_i - \tilde{m}[\theta]] \right\}_{\theta=\hat{\theta}} = 0 \quad (26)$$

where $\Re\{\cdot\}$ denotes taking the real part of a complex-valued function. To obtain a solution in a closed form, in practically all important cases, we consider that the solution of Equation (25) is determined by the first term for any given non-random parameter μ_i from the spatial region of the radiation source.

The obtained relations allow, after carrying out the corresponding calculations, to obtain the following optimal asymptotically efficient estimates of the signal amplitude A_i and the delay time τ_i .

$$\hat{\tau}_i = \underset{\tau}{\operatorname{argmax}} \left\{ \sum_{k=1}^N x_i(t_k) s(\tau + t_k) \right\} \tag{27}$$

$$\hat{A}_i = \left(\Re \left\{ \left[\tilde{\mathbf{S}} e^{-j\omega \hat{\tau}_i} \right]^H \tilde{\mathbf{X}}_i \right\} \right) / \tilde{\mathbf{S}}^H \tilde{\mathbf{S}} = \sum_{k=1}^N x_i(t_k) s(\hat{\tau} + t_k) / \sum_{k=1}^N s^2(t_k) \tag{28}$$

The optimal estimate of the signal delay time τ in accordance with relation (27) indicates that the value of the estimate τ coincides with the maximum of the correlation integral of the input signal $x(t)$ and the signal $s(t + \tau)$ with a variable time shift τ . When calculating the optimal amplitude estimate, the value of the delay time τ is considered to be a given value.

It is easy to show that the obtained estimates of the delay time τ and the signal amplitude A_i , as follows from the properties of the maximum a posteriori (MAP) estimate method [53,54], are unbiased and

$$M\{\hat{A}_i\} = A_i \tag{29}$$

4. CRLB for Estimating Delay Time and Signal Amplitude. Source Range Estimator

The root-mean-square errors (RMS) of the obtained optimal estimates of the parameters τ_i and A_i satisfy the Bayesian Cramer–Rao lower bound (BCRLB), and, for the sample size of the observed signal $N \rightarrow \infty$, BCRLB coincides with the RMS derivation due to the asymptotic efficiency of the MAP parameter estimation method. The error covariance matrix for estimating the parameters τ_i and A_i is determined by the Bayesian Information Matrix (BIM) \mathbf{J}_B with a size of 2×2 elements [53,54].

$$\mathbf{J}_B(\theta) = -M \left\{ \nabla_{\theta} \left[\nabla_{\theta} l_B(\theta, \tilde{\mathbf{X}}_i) \right]^T \right\} = M \left\{ \left[\nabla_{\theta} l_B(\theta, \tilde{\mathbf{X}}_i) \right] \left[\nabla_{\theta} l_B(\theta, \tilde{\mathbf{X}}_i) \right]^T \right\}, \tag{30}$$

where the Bayesian log-likelihood function l_B is defined by expression (20).

The calculation of the Bayesian lower bound of the covariance matrix of estimates \mathbf{C}_{ϵ} is based on the Cramer–Rao inequality.

$$\mathbf{C}_{\epsilon} \triangleq M \left\{ [\hat{\theta} - \theta]^H [\hat{\theta} - \theta] \right\} \geq \mathbf{J}_B^{-1}(\theta), \tag{31}$$

where $\mathbf{J}_B^{-1}(\theta)$ — is the matrix inverse to the Bayesian information matrix (29). The diagonal elements in the matrix (30) \mathbf{C}_{τ} and \mathbf{C}_A are equal to the lower Bayesian bound of the corresponding mean square errors of the parameter estimates, so the off-diagonal BIM elements $\mathbf{C}_{\tau,A}$ determine the error correlation.

With the mathematical model is used for describing the location system, the calculation of BIM leads to the following result:

$$\left[\mathbf{J}_B^{-1}(\theta) \right]_{\tau,A} = \left[\mathbf{J}_B^{-1}(\theta) \right]_{A,\tau} = 0, \tag{32}$$

i.e., the mutual errors in the estimates of the amplitude A_i and the signal delay time τ_i are not correlated.

The formulas for calculating the diagonal elements of the matrix C_ε for signals discrete in time have the form

$$C_A = \sigma_a^2 = \left[\frac{\sum_j |\tilde{S}(f_j)|^2}{\frac{1}{2} N_0 T_0} + \frac{1}{\sigma_{A_i}^2} \right]^{-1} = \left[\frac{\sum_j |s(t_j)|^2}{\sigma_n^2} + \frac{1}{\sigma_{A_i}^2} \right]^{-1}, \quad (33)$$

$$C_\tau = \sigma_\tau^2 = \frac{\sigma_n^2}{A_i^2 \sum_j \left| \frac{\partial s_i(t_j)}{\partial t} \right|^2}, \quad (34)$$

where, as before, the parameters σ_n and σ_A mean the magnitude of the receiver noise dispersion over the entire operating frequency range and the dispersion of the signal amplitude in the lognormal distribution (9) in the Gaussian approximation (10).

Consider the implementation of the algorithm for optimal estimation of distances r_1 and r_2 from the radiation source SN to the corresponding two base stations AN₁ and AN₂ (see Figure 1). Estimated parameters r_1 and r_2 are unknown and non-random values. During one measurement session, in accordance with the proposed algorithm (27), (28), the optimal asymptotically efficient unbiased estimates of the signal amplitudes A_1, A_2 , and the delay time difference τ_{12} . For the mathematical model of the measurement results, the vector $R \equiv [R_1, R_2, R_3]^T$ can be represented as:

$$R_1 = v_g (\hat{\tau}_1 - \hat{\tau}_2) = v_g \hat{\tau}_{12} = (r_1 - r_2) + n_1, \quad (35)$$

$$R_2 = \hat{A}_1 = A_1 + n_2, \quad (36)$$

$$R_3 = \hat{A}_2 = A_2 + n_3, \quad (37)$$

where v_g is the group velocity of signal propagation in the medium, and the measurement noise n_1, n_2 , and n_3 are centered random variables having normal probability distribution densities w_1, w_2 , and w_3 with parameters.

$$w_1 = \mathcal{N}(0, v_g^2 \sigma_\tau^2); \quad w_2 = w_3 = \mathcal{N}(0, \sigma_0^2), \quad (38)$$

The variance σ_τ^2 is determined by relation (33), and the variance σ_0^2 is determined by the first term in square brackets (32).

Random amplitudes A_1 and A_2 in the expressions have a log-normal distribution with parameters μ_1, μ_2 and σ_P^2 in accordance with (21). The proposed model allows us to determine the probability distribution densities p_1, p_2 , and p_3 of the measurement results R_1, R_2 , and R_3 :

$$p_1(R_1 | r_1 - r_2) = \frac{1}{v_g \sigma_\tau \sqrt{2\pi}} \exp \left[-\frac{1}{2v_g^2 \sigma_\tau^2} (R_1 - r_1 + r_2)^2 \right], \quad (39)$$

$$p_i(R_i | r_1, r_2) = \int_{-\infty}^{\infty} \frac{M_1}{A_i \sigma_P \sqrt{2\pi}} \exp \left[-\frac{1}{2} \frac{(\lg A_i - \mu_i)^2}{\sigma_P^2} \right] \frac{1}{\sigma_0 \sqrt{2\pi}} \exp \left[-\frac{1}{2\sigma_0^2} (R_i - A_i)^2 \right] dA_i, \quad i = 2, 3, \quad (40)$$

The probability distribution densities p_2 and p_3 in (39) are calculated through the convolution integral of the one-dimensional densities $w_{2,3}$ and $p_A(A_i)$ [56]. In practical applications, the inequality $\sigma_P \gg \sigma_0$ is usually satisfied. In this case, the probability distribution densities p_2 and p_3 approximately have a lognormal law (21).

To estimate the radii r_1 and r_2 as unknown but nonrandom parameters, we use the Maximum Likelihood (ML) strategy. This strategy is based on finding the maximum of the logarithm of the likelihood function $\ln l(R, r_1, r_2)$ and solving the likelihood equation [53,54]

for the two-dimensional case. Two scenarios are possible when developing a range estimator to a radiation source.

The first scenario—the transmitter power, and, hence, the amplitude of the signal A_0 at the reference point, are considered a priori given values. In this case, the estimate of the radii r_1 and r_2 follows from the solution of the system of equations:

$$\frac{\partial \ln l(\mathbf{R}, r_1, r_2)}{\partial r_i} = 0, \quad i = 1, 2, \quad (41)$$

$$\ln l(\mathbf{R}, r_1, r_2) = \ln p_1(R_1|r_1 - r_2) + \ln p_2(R_2|r_1, r_2) + \ln p_3(R_3|r_1, r_2), \quad (42)$$

The solution of the transcendental Equation (41) for the unknowns r_1 and r_2 can be carried out numerically or approximately by analytical methods. The analysis performed shows that due to the determination of two unknowns r_1 and r_2 from the results of three measurements R_1 , R_2 , and R_3 , the accuracy of determining the coordinates SN of the radiation source increases.

Let us consider in more detail the scenario when the transmitter power is not known a priori. This case is more common in practice, since the signal amplitude A_0 at the reference point depends on the radiation pattern of the receiver and transmitter antennas, technological deviations from the average values of the parameters of the devices that make up the network, and so on. In this case, it is advisable to choose the ratio R_1/R_2 as the result of the second measurement Y . Due to the fact that the random variables R_1 and R_2 have probability distribution densities close to log-normal, their ratio also has a log-normal distribution [49].

$$p_Y(Y|r_1, r_2) = p_Y\left(\frac{R_1}{R_2}|r_1, r_2\right) = \frac{M_1}{Y\sigma_P\sqrt{4\pi}} \exp\left[-\frac{1}{2} \frac{\left(\lg Y - \frac{\gamma}{2} \lg \frac{r_2}{r_1}\right)^2}{2\sigma_P^2}\right], \quad (43)$$

The estimation of the parameters r_1 and r_2 follows from the solution of the system of equations:

$$\frac{\partial \ln l(R_1, Y, r_1, r_2)}{\partial r_1} = 0, \quad \frac{\partial \ln l(R_1, Y, r_1, r_2)}{\partial r_2} = 0, \quad (44)$$

$$\ln l(R_1, Y, r_1, r_2) = \ln p_1(R_1|r_1 - r_2) + p_Y(Y|r_1, r_2), \quad (45)$$

The solution of the system of Equation (43) in the final (closed) form is possible when the value of the indicator γ of the signal attenuation during its propagation in the medium is equal to two. In this case

$$r_1 = \frac{R_1}{1 - Y}; \quad r_2 = \frac{R_1 Y}{1 - Y}, \quad (46)$$

Using the rule of approximate calculation of the mathematical expectation of a random variable, it is easy to obtain the statistical characteristics of the estimation of the parameters r_1 and r_2 [56].

$$M\{r_1\} \approx \frac{M\{R_1\}}{1 - M\{Y\}} = \frac{r_1 - r_2}{1 - \frac{r_2}{r_1}\alpha}, \quad (47)$$

$$M\{r_2\} \approx \frac{M\{R_1\} \cdot M\{Y\}}{1 - M\{Y\}} = \frac{(r_1 - r_2) \frac{r_2}{r_1} \alpha}{1 - \frac{r_2}{r_1}\alpha}, \quad (48)$$

In expressions (46) and (47), the parameter α is determined by the following relation:

$$\alpha = \exp\left(\sigma_{Pe}^2\right), \quad (49)$$

It follows from relations (46) and (47) that as the variance σ_p^2 tends to zero, the estimates of the parameters r_1 and r_2 are unbiased. With a finite value of the dispersion σ_p^2 , these estimates become biased.

Similarly, using the rule of approximate calculation of the variance of a random variable, it is easy to obtain the variance of the estimates of the parameters r_1 and r_2 [56].

$$\frac{D\{r_1\}}{r_1^2} = \frac{1}{\left(1 - \alpha \frac{r_2}{r_1}\right)^2} \left[\frac{2\sigma_\tau^2 v_g^2}{r_1^2} + \frac{\left(1 - \frac{r_2}{r_1}\right)^2 \left(\frac{r_2}{r_1}\right)^2}{\left(1 - \alpha \frac{r_2}{r_1}\right)^2} \alpha^2 (\alpha^2 - 1) \right], \quad (50)$$

$$\frac{D\{r_2\}}{r_2^2} = \frac{1}{\left(1 - \alpha \frac{r_2}{r_1}\right)^2} \left[\frac{2\sigma_\tau^2 v_g^2}{r_1^2} + \frac{\left(1 - \frac{r_2}{r_1}\right)^2}{\left(1 - \alpha \frac{r_2}{r_1}\right)^2} \alpha^2 (\alpha^2 - 1) \right], \quad (51)$$

Estimation of the parameters r_1 and r_2 in the general case does not lead to an unambiguous determination of the coordinates of the radiation source SN, since the radii r_1 and r_2 intersect at two spatial points symmetrically with respect to the base—the line connecting the two base stations AN₁ and AN₂ (see Figure 1). To unambiguously determine the SN coordinates, it is necessary that all sources are on the same side of the base.

5. Simulation Results and Discussion

To check the obtained theoretical results and the adequacy of the proposed mathematical models, a computer simulation (machine experiment) was carried out, during which the statistical characteristics of the obtained parameter estimates were determined. When performing the computer simulation, the selection of the numerical values of the parameters UWB of the Gaussian monocycle radio pulse, the time sampling frequency f_s , the number of samples in the signal sample N , and other parameters was based on the resource of modern and promising hardware as well as the corresponding technical implementations based on them.

The power of the SN transmitter was determined by the requirements of the USA Federal Communications Commission (FCC) and was minus 17 dBm during the simulation. This parameter corresponds to a power spectral density level of about minus 50 dBm/MHz in the frequency band from 3 to 10 GHz. The parameter τ of the UWB pulse was chosen to be 1.15 ns, which determined the effective operating bandwidth of the signal Δf_e equal to about 500 MHz. The number of samples in the signal sample N was chosen to be 1024 and 2048. This choice is dictated by the size of the memory buffer of modern high-speed processors. In addition, the value of N determines the sampling duration $T_0 = N/f_s$, and, consequently, the maximum range of MSNs for the R_{\max} at a given sampling rate. In modeling, the frequency $f_s \geq 2\Delta f_e$, which determines the time sampling step $\Delta t = 1/f_s$, was chosen to be 3 GHz and 6 GHz, which corresponded to 24 and 48 counts at the effective duration of a Gaussian unicycle. The value of r_1 in the simulation was chosen to be 33 m. To obtain the sample mean and sample variance of the proposed estimates, multiple repetitions of computer calculations were carried out for different implementations of noise, followed by statistical processing.

a shows the implementation of the input signal $x(t)$ with an SNR of 12 dB. Figure 4b shows the result of processing the signal $x(t)$, which implements a point estimate of the signal arrival time τ_t by the maximum of the function $R_x(\tau)$ defined by Formula (27). The $R_x(\tau)$ function as a random process has fluctuations (see Figure 4b), the level of which increases as the input noise increases (SNR decreases). When statistically processing a large number of a set of realizations, the probability P of a random event that the level of one individual sample $R_x(\tau)$ of the n -th realization will exceed the maximum value, and the

signal arrival time will be estimated in the sampling interval Δt_k anomalously far from τ_t , as determined by the formula

$$P = \operatorname{erf} \frac{\beta}{\sqrt{2}}, \quad (52)$$

where $\operatorname{erf}(\cdot)$ is the error function. In this case, the variance of the estimate increases sharply. When the value of the parameter β is less than 4.6, the probability of such an error is low. This condition imposes a restriction on the lower limit of the change in the SNR parameter for a point estimate of the signal arrival time, which turns out to be approximately 5 dB. With a smaller SNR value, it is necessary to use the methods of interval parameter estimation. The upper limit of the SNR parameter for a given transmitter power SN is determined by the distance to AN and the minimum possible noise figure of the receiver, which was assumed to be several decibels in the simulation in the absence of a cryogenic cooling system.

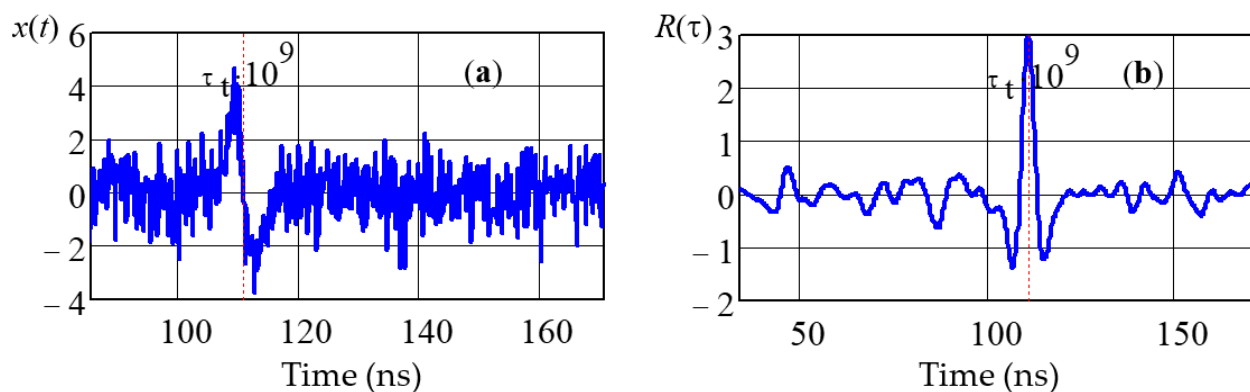


Figure 4. Implementation of the input signal $x(t)$ (a) and the output signal of the estimator (b).

Figure 5 shows a comparison of the dependences of the normalized standard deviations of the delay time estimate and the signal amplitude estimate on the SNR value for various values of the sample size $N = 1024$ and $N = 2048$. The blue color shows the graphs of the results of calculating the parameter estimates using the proposed algorithm (relations (27) and (28)), while in red are the plots of the Cramer–Rao lower bound of the corresponding estimate. As follows from the theoretical analysis, the estimate weakly depends on the sample size at a fixed value of the sampling rate f_s equal to 3 GHz and the UWB pulse parameter τ equal to 1.15 ns. The difference between the estimate of the signal arrival time τ_t and CRLB can be explained by the discrete nature of signal processing. A slight increase in the discrepancy between the obtained estimate and CRLB at $N = 2048$ is explained by an increase in the statistical error in determining sample estimates with an increase in the sample size.

Figure 6 shows a comparison of the dependences of the normalized standard deviations of the delay time estimate and the signal amplitude estimate on the SNR value for various values of the parameter τ_0 UWB of the Gaussian unicycle radio pulse equal to 1.15 ns and 2.25 ns. The sampling rate in the computer experiment is 6 GHz and the sample size is $N = 2048$. The blue graphs display the results of the parameters estimation calculation according to the proposed algorithm, while the graphs of the Cramer–Rao Lower Bound of the corresponding estimate are displayed in red. The better coincidence between the arrival time estimate and CRLB compared to the previous case is explained by the doubling of the number of readings in the Gaussian unicycle duration interval. The closeness of the proposed estimate to CRLB, obtained as a result of the simulation, confirms the conclusion about the asymptotic efficiency of the estimate obtained using the MAP strategy.

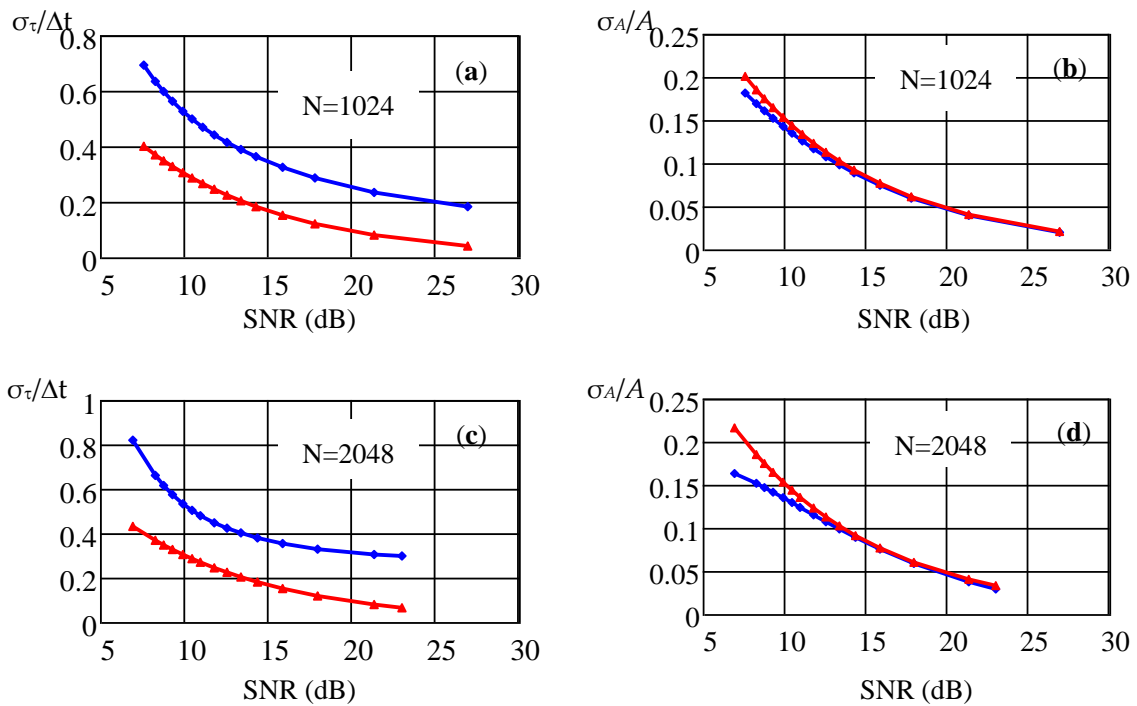


Figure 5. Dependences of the normalized standard deviations of the delay time estimate (a,c) and the signal amplitude estimate (b,d) on the SNR value for various parameter values $N = 1024$ and $N = 2048$, $f_s = 3$ GHz.

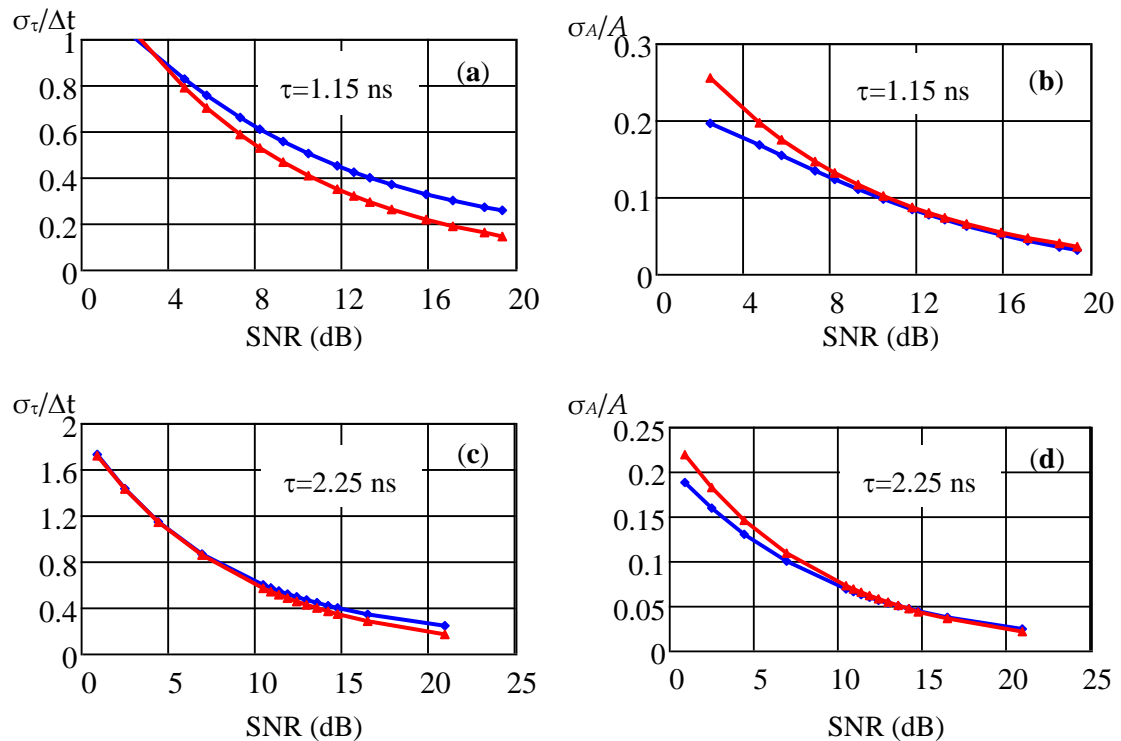


Figure 6. Dependences of the normalized standard deviations of the delay time estimate (a,c) and the signal amplitude estimate (b,d) on the SNR value for different values of the parameter $\tau = 1.15$ ns and $\tau = 2.25$ ns, $f_s = 6$ GHz.

Figure 7 shows the dependences of the normalized value of the average value of the estimate r_1 on the parameter σ^2_P and the two values of the ratio of radii. The estimate was normalized to the true value of the radius r_1 , the value of the parameter τ_0 is 1.15 ns, the sampling frequency is 6 GHz, and the sample size is $N = 2048$. As the ratio r_2/r_1 approaches unity, the shift in the estimate of the average value of the radius increases sharply with the growth of the variance of the lognormal distribution σ^2_P . The point $r_2/r_1 = 1$ is singular in Equations (46)–(50). Thus, for the value $\sigma^2_P = 1$ dB and the radius ratio $r_2/r_1 = 0.5$, the estimate shift reaches 40% (see Figure 7).

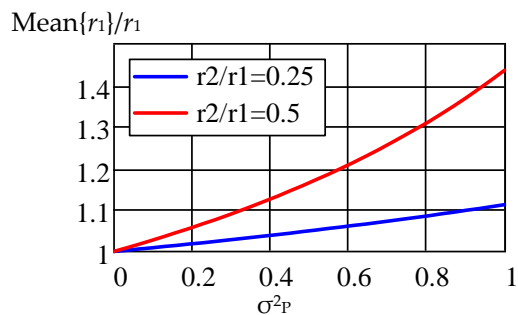


Figure 7. Dependence of the normalized value of the average value of the estimate r_1 on the parameter σ^2_P for two values of the ratio of radii r_2/r_1 .

In Figure 8, dependences of the normalized standard deviation of the estimate r_1 on the parameter σ^2_P (a) and the SNR parameter (b) are presented. The estimate was normalized to the true value of the radius r_1 , the value of the parameter τ_0 is 1.15 ns, the sampling frequency is 6 GHz, and the sample size is $N = 2048$. The dependence on the parameter σ^2_P is given for two ratios of radii $r_2/r_1 = 0.25$ and $r_2/r_1 = 0.5$. The dependence on the SNR parameter is given for two values of the dispersion σ^2_P , the blue graph corresponds to the case $\sigma^2_P \approx 0$ and the red curve to the case $\sigma^2_P \approx 0.3 \cdot 10^{-3}$ dB, with the radius ratio $r_2/r_1 = 0.2$. As well as the bias of the radius estimate, the variance of the estimate increases sharply as the parameter r_2/r_1 approaches one. The simulation results show in this case, that when the variance of the lognormal distribution exceeds $\sigma^2_b = 10^{-3}$ dB, the main source of error in estimating the distance to AS is the statistical properties of the propagation medium of the UWB signal in the LOS channel.

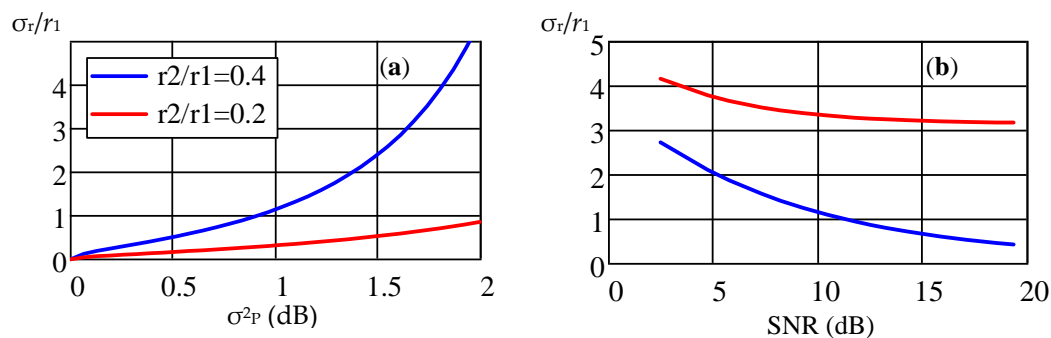


Figure 8. Dependences of the normalized standard deviation σ_r/r_1 of the estimate r_1 on the parameter σ^2_P (a) and the SNR ratio (b).

Figure 9 shows 3D graphs of the statistical characteristics of the estimates of the radius r_1 , calculated by relations (46) and (49). The simulation parameters are chosen identically, in which the dependences presented in Figure 8 were calculated. As follows from relations (46) and (49) and, accordingly, from the graphs in Figure 9, the bias of the estimate (a) and the standard deviation of the estimate of the parameter r_1 (b) begin to increase with increasing noise dispersion of the amplitude σ^2_P in the logarithmic

normal distribution (42), tending to be the ratio of radii r_2/r_1 to one. When deriving Formulas (45)–(50), it was assumed that the ratio r_2/r_1 is not equal to 1 one.

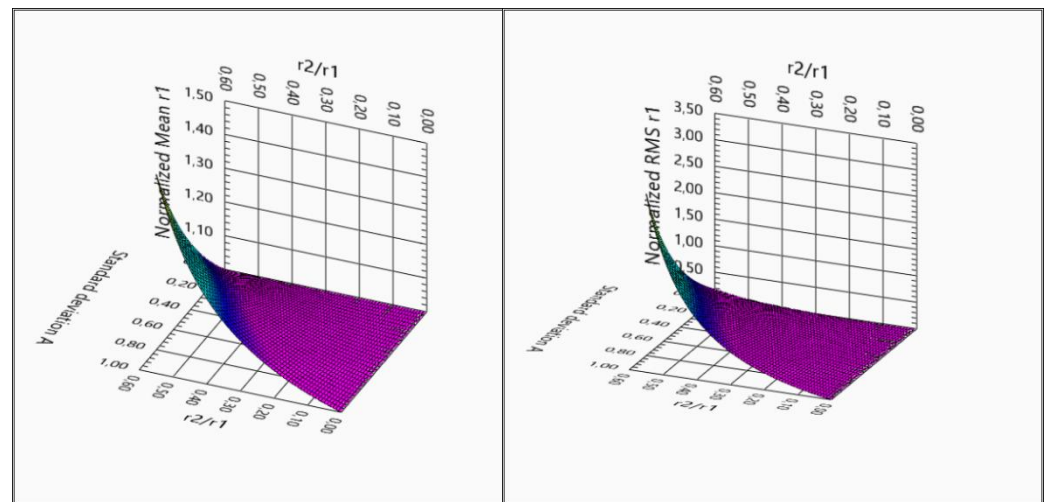


Figure 9. The 3D dependences of the normalized value of the mean value (a) and the normalized standard deviation of the estimate r_1 (b) on the parameter σ_p^2 and the ratio of radii r_2/r_1 .

The statistical characteristics of the estimate of the radius r_2 are similar to those for the radius r_1 . The obtained characteristics make it possible to determine the maximum value of the parameter σ_p^2 and the operating interval of the ratios r_2/r_1 by the given allowable values of the bias and standard deviation of the range estimate. It is also possible to solve the inverse problem by the given value of the parameter σ_p^2 and the working interval of the ratios r_2/r_1 to determine the values of the offset and the standard deviation of the range estimate.

6. Conclusions

The use of hybrid methods, such as RSS/TDoA, can improve the statistical characteristics of the spatial positioning of radio sources using Microwave Sensors Networks (MSN). One effective way to deal with multipath fading, including in small enclosed spaces, is to use UWB pulsed radio systems, due to their high time resolution capability. The work proposes a statistical model of a radio channel that adequately describes the propagation of a UWB signal under Line of Sight conditions and allows a closed-ended theoretical analysis and further computer simulation of the MSN statistical characteristics. For the first time, an algorithm for estimating the parameters of the spatial positioning of radio sources is proposed, taking into account a priori data on the logarithmically normal probability distribution density of a random value of the power UWB of a pulse signal, when it propagates in a medium with given statistical properties. The computer simulation performed showed that the dispersion of the obtained optimal estimate of the amplitude A_i and the signal propagation delay time τ based on the Bayesian strategy of maximum a posteriori probability in the operating range of the input noise level of the receiver are close to the Bayesian Cramer–Rao Lower Bound (BCRLB). For a scenario with an a priori unknown value of the transmitter power of the radiation source, an algorithm has been developed for optimal estimation of the distances from the source to the base stations based on the results of measurements of the amplitude and propagation delay time of the UWB radio signal. It is shown that when the variance of the log-normal distribution exceeds σ_b^2 (the value of σ_b^2 depends on the MSN parameters), the main source of error in estimating the distance to AS is the statistical properties of the propagation medium of the UWB signal in the LOS channel. The bias and variance of the obtained estimate of the distance from the source to the base stations increase with increasing distance, the noise level of the receiver, and the parameter σ_p of the of the log-normal distribution of the UWB signal power. An increase in

the bias and variance of the obtained estimate is also observed when the value of the ratio of radii r_2/r_1 approaches a value equal to one. This evaluation behavior is related to the method of solving the system of equations and may be solved by a modified method in the future.

For further work, it is planned to refine the developed algorithm for estimating parameters in the presence of multiple radar targets and several base stations, as well as algorithms, for tracking the trajectory of unmanned vehicles with subsequent filtering algorithms. The mode of operation of an automotive radar in conditions of multiple radar targets and monitoring indoors of a limited volume is important in the practical use of the algorithm in modern driver assistance systems (ADAS—Advanced Driver Assistance System) to ensure the most comfortable and safe vehicle movement, including in the fully autonomous (unmanned) mode of vehicle movement. Moreover, for further work to validate the integrity of approaches to analyzing the performance of the developed algorithm, it is planned to develop an experimental setup of a hardware-software complex for the radio-frequency positioning of objects, based on research results [57] and completed comparative test measurements.

Author Contributions: Conceptualization and formal analysis, S.I. and V.K.; investigation and validation, V.B. and A.F. All authors discussed and designed the proposed algorithm. All authors have read and agreed to the published version of the manuscript.

Funding: The reported study was funded by RFBR, project number 19-29-06034.

Institutional Review Board Statement: Not applicable.

Informed Consent Statement: Not applicable.

Data Availability Statement: Not applicable.

Conflicts of Interest: The authors declare no conflict of interest.

References

1. Zekavat, S.A.; Buehrer, R.M. (Eds.) *Handbook of Position Location Theory, Practice, and Advances*; John Wiley&Sons, Inc.: Hoboken, NJ, USA, 2019; Chapter 1; pp. 3–24.
2. Chen, Y.-S.; Hsu, C.-S.; Chung, R.-S. A Semi-Supervised 3D Indoor Localization Using Multi-Kernel Learning for WiFi Networks. *Sensors* **2022**, *22*, 776. [[CrossRef](#)] [[PubMed](#)]
3. Xu, F.; Hu, X.; Shuaiwei Luo, S.; Shang, J. An Efficient Indoor Wi-Fi Positioning Method Using Virtual Location of AP. *ISPRS Int. J. Geo-Inf.* **2020**, *9*, 261. [[CrossRef](#)]
4. Zhao, K.; Zhao, T.; Zheng, Z.; Yu, C.; Ma, D.; Rabie, K.; Kharel, R. Optimization of Time Synchronization and Algorithms with TDOA Based Indoor Positioning Technique for Internet of Things. *Sensors* **2020**, *20*, 6513. [[CrossRef](#)] [[PubMed](#)]
5. Kuptsov, V.D.; Badenko, V.L.; Ivanov, S.I.; Fedotov, A.A. Method for remote determination of object coordinates in space based on exact analytical solution of hyperbolic equations. *Sensors* **2020**, *20*, 5472. [[CrossRef](#)]
6. Patwari, N.; Ash, J.N.; Kyperountas, S.; Hero, A.O.; Moses, R.L.; Correal, N.S. Locating the nodes: Cooperative localization in wireless sensor networks. *IEEE Signal Process. Mag.* **2005**, *22*, 54–69. [[CrossRef](#)]
7. Patwari, N.; Hero, A.O.; Perkins, M.; Correal, N.S.; O’Dea, J. Relative location estimation in wireless sensor networks. *IEEE Trans. Signal Process.* **2003**, *51*, 2137–2148. [[CrossRef](#)]
8. Shen, J.; Molisch, A.F.; Salmi, J. Accurate passive location estimation using TOA measurements. *IEEE Trans. Wirel. Commun.* **2002**, *11*, 2182–2192. [[CrossRef](#)]
9. Chan, Y.T.; Tsui, W.; So, H.; Ching, P. Time-of-arrival based localization under NLOS conditions. *IEEE Trans. Veh. Technol.* **2006**, *55*, 17–24. [[CrossRef](#)]
10. Yang, L.; Ho, K.C. An Approximately Efficient TDOA Localization Algorithm in Closed-Form for Locating Multiple Disjoint Sources with Erroneous Sensor Positions. *IEEE Trans. Signal Process.* **2009**, *57*, 4598–4615. [[CrossRef](#)]
11. Vankayalapati, N.; Kay, S.; Ding, Q. TDOA based direct positioning maximum likelihood estimator and the Cramer Rao bound. *IEEE Trans. Aerosp. Electron. Syst.* **2014**, *55*, 1616–1635. [[CrossRef](#)]
12. So, H.C.; Lin, L. Linear least squares approach for accurate received signal strength based source localization. *IEEE Trans. Signal Process.* **2011**, *59*, 4035–4040. [[CrossRef](#)]
13. Lin, L.; So, H.C.; Chan, Y.T. Received signal strength based positioning for multiple nodes in wireless sensor networks. *Digit. Signal Process.* **2014**, *25*, 41–50. [[CrossRef](#)]
14. Li, X. Collaborative localization with received-signal strength in wireless sensor networks. *IEEE Trans. Veh. Technol.* **2007**, *56*, 3807–3817. [[CrossRef](#)]

15. Ho, K.C.; Lu, X.; Kovavisaruch, L. Source localization using TDOA and FDOA measurements in the presence of receiver location errors: Analysis and solution. *IEEE Trans. Signal Process.* **2007**, *55*, 684–696. [[CrossRef](#)]
16. Yin, J.; Wan, Q.; Yang, S.; Ho, K.C. A Simple and Accurate TDOA-AOA Localization Method Using Two Stations. *IEEE Signal Process. Lett.* **2016**, *23*, 144–148. [[CrossRef](#)]
17. Tranter, W.H.; Shanmugan, K.S.; Rappaport, T.S.; Kosbar, K.L. *Principles of Communication Systems Simulation with Wireless Applications*; PTR: Prentice Hall, NJ, USA, 2003; Chapters 14; pp. 529–582.
18. Saleh, A.A.M.; Valenzuela, R. A Statistical Model for Indoor Multipath Propagation. *IEEE J. Sel. Areas Commun.* **1987**, *5*, 128–137. [[CrossRef](#)]
19. Win, M.Z.; Scholtz, R.A. On the robustness of ultra-wide bandwidth signals in dense multipath environments. *IEEE Commun. Lett.* **1998**, *2*, 51–53. [[CrossRef](#)]
20. Karedal, J.; Wyne, S.; Almers, P.; Tufvesson, F.; Molisch, A.F. UWB Channel Measurements in an Industrial Environment. In Proceedings of the IEEE Global Telecommunications Conference, GLOBECOM '04, Dallas, TX, USA, 29 November–3 December 2004; pp. 3511–3516. [[CrossRef](#)]
21. Molisch, A.F.; Balakrishnan, K.; Cassioli, D.; Chong, C.-C.; Emami, S.; Fort, A.; Karedal, J.; Kunisch, J.; Schantz, H.; Siwiak, K. A comprehensive model for ultrawideband propagation channels. GLOBECOM 05. In Proceedings of the IEEE Global Telecommunications Conference, St. Louis, MO, USA, 28 November–2 December 2005; pp. 3648–3653. [[CrossRef](#)]
22. Molisch, A.F.; Foerster, J.R.; Pendergrass, M. Channel models for ultra-wideband personal area networks. *IEEE Wirel. Commun. Mag.* **2003**, *10*, 14–21. [[CrossRef](#)]
23. Foerster, J. Channel Modelling Sub-Committee Report Final (doc.: IEEE 802-15-02/490r1-SG3a), Submitted to IEEE P802.15 Working Group for Wireless Personal Area Networks (WPANs). 2002. Available online: <http://grouper.ieee.org/groups/802/15/pub/2002/Nov02/> (accessed on 28 February 2022).
24. Molisch, A.F.; Balakrishnan, K.; Chong, C.-C.; Emami, S.; Fort, A.; Karedal, J.; Kunisch, J.; Schantz, H.; Schuster, U.; Siwiak, K. *IEEE 802.15.4a Channel Model—Final Report, IEEE Standards Documents*; IEEE: Piscataway, NJ, USA, 2004; Volume 15, pp. 1–40.
25. Alavi, A.B.; Pahlavan, K. Modeling of the TOA based Distance Measurement Error Using UWB Indoor Radio Measurements. *IEEE Commun. Lett.* **2006**, *10*, 275–277. [[CrossRef](#)]
26. Hatami, A.; Pahlavan, K.; Heidari, M.; Akgul, F. On RSS and TOA based Indoor Geolocation—A Comparative Performance Evaluation. In Proceedings of the IEEE Wireless Communications and Networking Conference, WCNC, Doha, Qatar, 3–6 April 2006; pp. 2267–2272. [[CrossRef](#)]
27. Hatami, A.; Pahlavan, K. Performance Comparison of RSS and TOA Indoor Geolocation Based on UWB Measurement of Channel Characteristics. In Proceedings of the 2006 IEEE 17th International Symposium on Personal, Indoor and Mobile Radio Communications, Helsinki, Finland, 11–14 September 2006; pp. 1–6. [[CrossRef](#)]
28. Huang, B.; Xie, L.; Yang, Z. TDOA-Based Source Localization with Distance-Dependent Noises. *IEEE Trans. Wirel. Commun.* **2015**, *14*, 468–480. [[CrossRef](#)]
29. Catovic, A.; Sahinoglu, Z. The Cramer-Rao bounds of hybrid TOA/RSS and TDOA/RSS location estimation schemes. *IEEE Commun. Lett.* **2004**, *8*, 626–628. [[CrossRef](#)]
30. Huang, J.-Y.; Wan, Q. Comments on The Cramer-Rao Bounds of Hybrid TOA/RSS and TDOA/RSS Location Estimation Schemes. *IEEE Commun. Lett.* **2007**, *11*, 848–849. [[CrossRef](#)]
31. Ho, K.C.; Sun, M. Passive Source Localization Using Time Differences of Arrival and Gain Ratios of Arrival. *IEEE Trans. Signal Process.* **2008**, *56*, 464–477. [[CrossRef](#)]
32. Pahlavan, K.; Akgul, F.O.; Heidari, M.; Hatami, A.; Elwell, J.M.; Tingley, R.D. Indoor geolocation in the absence of direct path. *IEEE Wirel. Commun.* **2006**, *13*, 50–58. [[CrossRef](#)]
33. Alsindi, N.; Li, X.; Pahlavan, K. Analysis of Time of Arrival Estimation Using Wideband Measurements of Indoor Radio Propagations. *IEEE Trans. Instrum. Meas.* **2007**, *56*, 1537–1545. [[CrossRef](#)]
34. Alsindi, N.; Alavi, B.; Pahlavan, K. Spatial Characteristics of UWB TOA-based Ranging in Indoor Multipath Environments. In Proceedings of the IEEE 18th International Symposium on Personal, Indoor and Mobile Radio Communications, Athens, Greece, 3–7 September 2007; pp. 1–6. [[CrossRef](#)]
35. Maranò, S.; Gifford, W.M.; Wymeersch, H.; Win, M.Z. NLOS identification and mitigation for localization based on UWB experimental data. *IEEE J. Sel. Areas Commun.* **2010**, *28*, 1026–1035. [[CrossRef](#)]
36. Xiao, Z.; Wen, H.; Markham, A.; Trigoni, N.; Blunsom, P.; Frolik, J. Non-Line-of-Sight Identification and Mitigation Using Received Signal Strength. *IEEE Trans. Wirel. Commun.* **2015**, *14*, 1689–1702. [[CrossRef](#)]
37. Jin, D.; Yin, F.; Fritsche, C.; Gustafsson, F.; Zoubi, A.M. Bayesian Cooperative Localization Using Received Signal Strength with Unknown Path Loss Exponent: Message Passing Approaches. *IEEE Trans. Signal Process.* **2020**, *68*, 1120–1135. [[CrossRef](#)]
38. Coluccia, A.; Fascista, A. On the Hybrid TOA/RSS Range Estimation in Wireless Sensor Networks. *IEEE Trans. Wirel. Commun.* **2018**, *17*, 361–371. [[CrossRef](#)]
39. Katwe, M.; Ghare, P.; Sharma, P.K.; Kothari, A. NLOS Error Mitigation in Hybrid RSS-TOA-Based Localization through Semi-Definite Relaxation. *IEEE Commun. Lett.* **2020**, *24*, 2761–2765. [[CrossRef](#)]
40. Zuo, P.; Zhang, H.; Wang, C.; Jiang, H.; Pan, B. Directional Target Localization in NLOS Environments Using RSS-TOA Combined Measurements. *IEEE Wirel. Commun. Lett.* **2021**, *10*, 2602–2606. [[CrossRef](#)]

41. Tomic, S.; Beko, M.; Tuba, M.; Correia, V.M.F. Target Localization in NLOS Environments Using RSS and TOA Measurements. *IEEE Wirel. Commun. Lett.* **2018**, *7*, 1062–1065. [[CrossRef](#)]
42. Tomic, S.; Beko, M. A Robust NLOS Bias Mitigation Technique for RSS-TOA-Based Target Localization. *IEEE Signal Process. Lett.* **2019**, *26*, 64–68. [[CrossRef](#)]
43. Wann, C.-D.; Chin, H.-C. Hybrid TOA/RSSI Wireless Location with Unconstrained Nonlinear Optimization for Indoor UWB Channels. In Proceedings of the 2007 IEEE Wireless Communications and Networking Conference, Hong Kong, China, 11–15 March 2007; pp. 3943–3948. [[CrossRef](#)]
44. Laaraiedh, M.; Avrillon, S.; Uguen, B. Hybrid Data Fusion techniques for localization in UWB networks. In Proceedings of the 6th Workshop on Positioning, Navigation and Communication, Hannover, Germany, 19 March 2009; pp. 51–57. [[CrossRef](#)]
45. Hatami, A.; Pahlavan, K. QRPP1-5: Hybrid TOA-RSS Based Localization Using Neural Networks. In Proceedings of the 2006 IEEE Globecom, San Francisco, CA, USA, 27 November–1 December 2006; pp. 1–5. [[CrossRef](#)]
46. Ivanov, S.I.; Kuptsov, V.D.; Fedotov, A.A.; Badenko, V.L. Radio signal time delay estimation performance of TDOA/SSR-based source localization systems. *J. Phys. Conf. Ser.* **2021**, *2131*, 052062. [[CrossRef](#)]
47. Zhang, X.; Ying, W.; Yang, P.; Sun, M. Parameter estimation of underwater impulsive noise with the Class B model. *IET Radar Sonar Navig.* **2020**, *14*, 1055–1060. [[CrossRef](#)]
48. Gajo, Z. *Some Remarks on Maximum Likelihood Estimation in Alpha-Stable Environment*; Baltic URSI Symposium (URSI): Warsaw, Poland, 2020; pp. 1–2.
49. Aitchison, J.; Brown, J.A.C. *The Lognormal Distribution*; Cambridge at the University Press: Cambridge, UK, 1963; Chapter 2, pp. 7–17.
50. IEEE Std 802. *IEEE Std 802.15.4-2015 (Revision of IEEE Std 802.15.4-2011)*; IEEE Standard for Low-Rate Wireless Networks. IEEE: Piscataway, NJ, USA, 2016; pp. 1–709. [[CrossRef](#)]
51. US Federal Communications Commission (FCC), Part 15. 2003. Available online: <https://www.ecfr.gov/current/title-47/chapter-I/subchapter-A/part-15> (accessed on 28 February 2022).
52. Korn, G.A.; Korn, T.M. *Mathematical Handbook for Scientists and Engineers*; McGraw-Hill Book Company: New York, NY, USA, 1968.
53. Van Trees, H.L.; Bell, K.L.; Zhi, T. *Detection, Estimation, and Modulation Theory Part I: Detection, Estimation, and Filtering Theory*; John Wiley&Sons, Inc.: Hoboken, NJ, USA, 2013; Chapters 4 and 5; pp. 230–518.
54. Kay, S.M. *Fundamentals of Statistical Signal Processing: Estimation Theory*; PTR Upper Saddle River: Prentice Hall, NJ, USA, 1993; Chapter 11, pp. 341–378; Chapter 15, pp. 493–566.
55. Ivanov, S.I.; Kuptsov, V.D.; Fedotov, A.A.; Badenko, V.L. CFAR multi-target detection based on non-central Chi-square distribution for FMCW. *J. Phys. Conf. Ser.* **2020**, *1515*, 032059. [[CrossRef](#)]
56. Lloyd, E.; Ledermann, W. *Handbook of Applicable Mathematics. Volume VI: Statistics*; John Wiley&Sons Ltd.: Chichester, UK; New York, NY, USA, 1984; Chapter 2; pp. 66–73.
57. Badenko, V.; Antonov, A.; Fedotov, A.; Lei, Z.; Garg, R.D. Radio-frequency positioning methods for solving the problem of high precision 2D positioning. In Proceedings of the 2020 IOP Conference Series: Materials Science and Engineering, Chennai, India, 16–17 September 2020; Volume 953, p. 012083. [[CrossRef](#)]